CEBAF Program Advisory Committee Ten Proposal Cover Sheet

This document must be received by close of business on Tuesday, December 19, 1995 at:

CEBAF

User Liaison Office, Mail Stop 12 B

12000 Jefferson Avenue

Newport News, VA 23606

(Choose one)

☒ **New Proposal Title:** Precise Measurements of the Inclusive Spin-dependent Quasi-elastic Transverse Asymmetry $A_{T'}$ from $^3\vec{He}(\vec{e}, e')$ at low Q^2

☐ **Update Experiment Number:**

☐ **Letter-of-Intent Title:**

Contact Person

Name: Haiyan Gao

Institution: Univ. of Illinois at Urbana-Champaign

Address: Nuclear Physics Laboratory

Address: 1110 W. Green St.

City, State ZIP/Country: Urbana, IL 61801

Phone: (217) 333-5264 **FAX:** (217) 333-1215

E-Mail → Internet:

Experimental Hall: A **Days Requested for Approval:** 15

CEBAF Use Only

Receipt Date: 12/15/95 95-001

By: gp

LAB RESOURCES REQUIREMENTS LIST

CEBAF Proposal No.: _____ Date: _____
(For CEBAF User Liaison Office use only.)

List below significant resources — both equipment and human — that you are requesting *from CEBAF* in support of mounting and executing the proposed experiment. Do not include items that will be routinely supplied to all running experiments, such as the base equipment for the hall and technical support for routine operation, installation, and maintenance.

Major Installations *(either your equip. or new equip. requested from CEBAF)*

Polarized $^3\vec{H}e$ target

New Support Structures: _____

Data Acquisition/Reduction

Computing Resources: _____

New Software: _____

Major Equipment

Magnets _____

Power Supplies _____

Targets _____

Detectors _____

Electronics _____

Computer Hardware _____

Other _____

Other

BEAM REQUIREMENTS LIST

CEBAF Proposal No.:_____ Date: _____
(For CEBAF User Liaison Office use only.)

List all combinations of anticipated targets and beam conditions required to execute the experiment. (This list will form the primary basis for the Radiation Safety Assesment Document (RSAD) calculations that must be performed for each experiment.)

Condition #	Beam Energy (MeV)	Beam Current (μA)	Polarization and Other Special Requirements (e.g., time structure)	Target Material (use multiple rows for complex targets — e.g., w/windows)	Target Material Thickness (mg/cm²)
1	800	5-10μA	Polarized beam	^{3}He gas	50.1
2	1600	10 μA	Polarized beam	^{3}He gas	50.1

The beam energies, E_{Beam}, available are: $E_{Beam} = N \times E_{Linac}$ where N = 1, 2, 3, 4, or 5. For 1995, E_{Linac} = 800 MeV, i.e., available E_{Beam} are 800, 1600, 2400, 3200, and 4000 MeV. Starting in 1996, in an evolutionary way (and not necessarily in the order given) the following additional values of E_{Linac} will become available: E_{Linac} = 400, 500, 600, 700, 900, 1000, 1100, and 1200 MeV. The sequence and timing of the available resultant energies, E_{Beam}, will be determined by physics priorities and technical capabilities.

HAZARD IDENTIFICATION CHECKLIST

CEBAF Experiment: _____ Date: _____

Check all items for which there is an anticipated need—do not check items that are part of the CEBAF standard experiment (HRSE, HRSH, CLAS, HMS, SOS in standard configurations).

Cryogenics
- _____ beamline magnets
- _____ analysis magnets
- _____ target
- _____ drift chambers
- _____ other

Electrical Equipment
- _____ cryo/electrical devices
- _____ capacitor banks
- _____ high voltage
- _____ exposed equipment

Radioactive/Hazardous Materials
List any radioactive or hazadorous/ toxic materials planned for use:
_____
_____

Pressure Vessels
- _____ inside diameter
- _____ operating pressure
- _____ window material
- _____ window thickness

Flammable Gas or Liquids
(incl. target)
type: _____
flow rate: _____
capacity: _____

Other Target Materials
- ___ Beryllium (Be)
- ___ Lithium (Li)
- ___ Mercury (Hg)
- ___ Lead (Pb)
- ___ Tungsten (W)
- ___ Uranium (U)
- X Other (list below)

^3He gas, Rb, N_2

Vacuum Vessels
- _____ inside diameter
- _____ operating pressure
- _____ window material
- _____ window thickness

Radioactive Sources
- _____ permanent installation
- _____ temporary use

type: _____
strength: _____

Large Mech. Structure/System
- _____ lifting devices
- _____ motion controllers
- _____ scaffolding or elevated platforms
- _____ other

Lasers
type: Laser Diode System
wattage: 40-80 - W
class: CLASS IV

Installation
- X permanent for this
- _____ temporary experiment

Use
- _____ calibration
- _____ alignment

for the target

Hazardous Materials
- ___ cyanide plating materials
- ___ scintillation oil (from)
- ___ PCBs
- ___ methane
- ___ TMAE
- ___ TEA
- ___ photographic developers
- ___ other (list below)

_____
_____
_____

Notes:
_____
_____
_____
_____
_____
_____

Precise Measurements of the Inclusive Spin-dependent Quasi-elastic Transverse Asymmetry $A_{T'}$ from $^3\vec{H}e(\vec{e},e')$ at low Q^2

D.H. Beck, H. Gao (spokesperson), R.J. Holt, R.M. Laszewski,
M.A. Miller, A.M. Nathan, N. Simicevic, S.E. Williamson
UNIVERSITY OF ILLINOIS AT URBANA-CHAMPAIGN

Todd Averett, B.W. Filippone, E. Hughes, W. Korsch, R.D. McKeown, M. Pitt
CALIFORNIA INSTITUTE OF TECHNOLOGY

J.P. Chen, J. Gomez, J. LeRose, R. Michaels, E. Offerman,
S. Nanda, A. Saha, B. Wojtsekhowski
CONTINUOUS ELECTRON BEAM ACCELERATOR FACILITY

B. Anderson, D.M. Manley, G.G. Petratos, J. Watson
KENT STATE UNIVERSITY

G.D. Cates, K. Kumar, P. Bgorad, H. Middleton
PRINCETON UNIVERSITY

P.A. Souder, R. Holmes, J. McCracken, X. Wang
SYRACUSE UNIVERSITY

L. Auerbach, Z.-E. Meziani, K. Slifer
TEMPLE UNIVERSITY

Abstract

Polarized ^{3}He targets have proven to be a useful tool for studying the electric and magnetic form factors of the neutron, and the spin structure of the neutron. We propose for the first time to systematically measure the inclusive ^{3}He quasi-elastic transverse asymmetry, $A_{T'}$, at Q^2 = 0.1, 0.2, 0.3, 0.4, 0.5 (GeV/c)^2 with high statistical and systematic accuracy. A 2% statistical uncertainty is aimed at all the proposed values of Q^2, and 3% systematic uncertainty for $A_{T'}$ can be achieved for this experiment. The precise data will constrain theoretical calculations of ^{3}He quasi-elastic asymmetry. Furthermore, the neutron magentic form factor at Q^2 = 0.1, 0.2, 0.3, 0.4, 0.5 (GeV/c)^2 will be extracted from the measured asymmetries with an overall uncertainty of 2%. Precise measurements of G_M^n at low Q^2 will resolve the discrepancy among the existing data in the same Q^2 region.

I. INTRODUCTION AND PHYSICS MOTIVATIONS

Electromagnetic form factors are of fundamental importance for an understanding of the underlying structure of nucleons. Knowledge of the distribution of charge and magnetization within the nucleons provides a sensitive test of models based on QCD, as well as a basis for calculations of processes involving the electro-magnetic interaction with complex nuclei. Recently, there have been great interests in measuring the neutron magnetic form factor at low Q^2 using deuteron targets [1-3], motivated largely by the poor quality of the previous data on G_M^n at low Q^2 and also by the growing interests in measuring G_E^n at low Q^2. Fig. 1 shows the world data on the neutron magnetic form factor in the low Q^2 region. Fig. 2 shows the data on G_M^n at low Q^2 from recent measurements [1-3,11]. These recent measurements [1-3] have greatly reduced the statistical and systematic uncertainties associated with experiments using deuteron targets. Nevertheless, as shown in Fig. 2 large discrepancy exists among these measurements in the same Q^2 region. Also, the data by Bruins *et al.* [3] seem to indicate very different Q^2-dependence of G_M^n in the low Q^2 region from that of Markowitz *et al.* [1], as well as the Q^2-dependence of G_M^p in the same Q^2 region.

Precise measurements of the neutron magnetic form factor at low Q^2 is also very important in terms of determining the strange magnetic and electric form factor of the nucleon, $G_M^{(s)}$ and $G_E^{(s)}$ from parity-violation experiments. For e-p elastic scattering at backward-angle, up to radiative corrections G_M^n and $G_M^{(s)}$ enter the parity-violating asymmetry with equal weight [12]. Thus, an accurate extraction of $G_M^{(s)}$ requires very accurate knowledge of G_M^n. Likewise as far as a determination of $G_E^{(s)}$ is concerned for e-p elastic scattering at forward angle, the error in G_M^n is roughly three times more important than the uncertainty in G_E^n because of the premultiplying factor of μ_p in the parity-violating asymmetry [12].

FIGURES

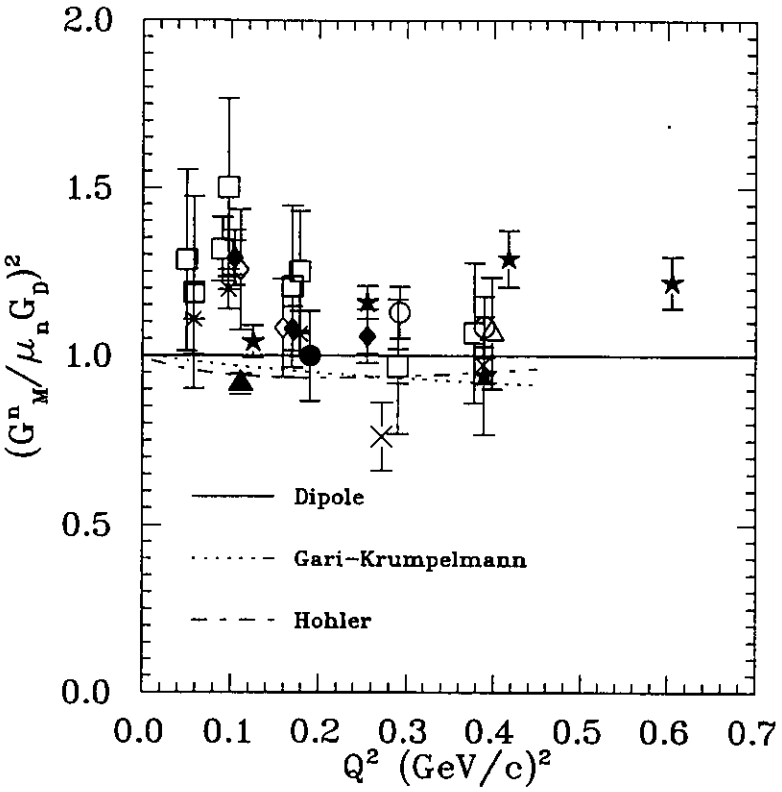

FIG. 1. The square of the neutron magnetic form factor $G_M^n{}^2$, in units of the standard dipole parametrization, $(\mu_n G_D)^2$, in the low Q^2 region. The open squares are from Hughes *et al.* [4], the open diamonds are from the analysis by Kramer *et al.* [5] of the data from Grossetête *et al.* [6], the asterisks are from Braess *et al.* [5], the crosses are from Hanson *et al.* [7], the open circles are from Budnitz *et al.* [8], the star is from Bartel *et al.* [9], the triangle is from Stein *et al.* [10], and the solid diamonds are from Markowitz *et al.* [1] with the inner (outer) error bars being the statistical (total) uncertainties. The solid triangle shows the result from Anklin *et al.* [2] with the total error being the quadrature sum of the statistical and systematic errors, the solid diamonds are from Bruins *et al.* [3] with the inner (outer) error bars being the statistical (total) uncertainties. The solid circle is from Gao *et al.* [11] shown with the total uncertainty dominated by the statistical error. The data of Markowitz *et al.*, Hughes *et al.*, and Stein *et al.* have been displaced slightly to improve readability.

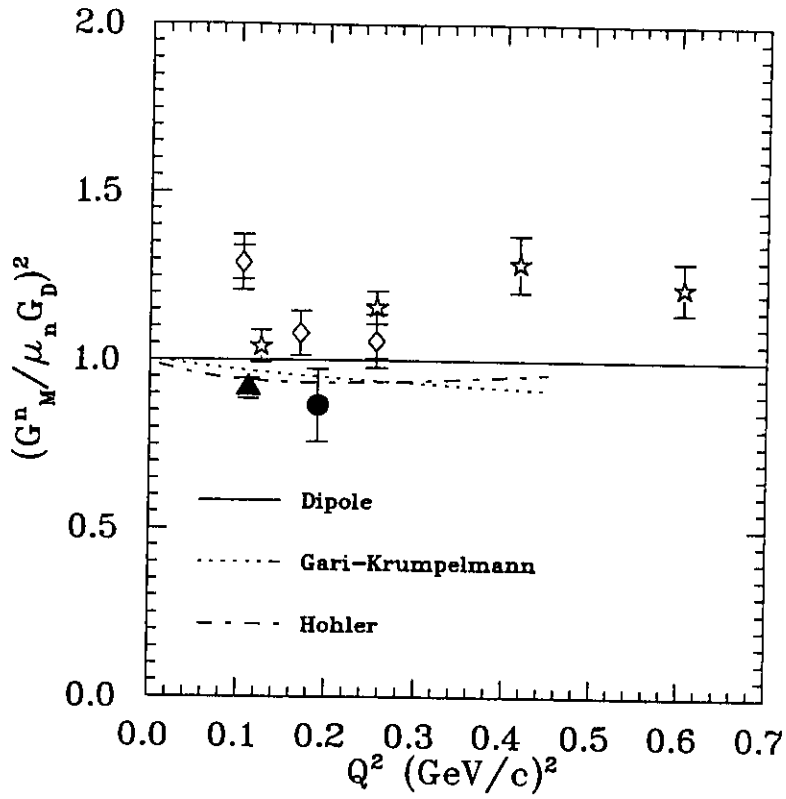

FIG. 2. **The square of the neutron magnetic form factor $G_M^n{}^2$, in units of the standard dipole parametrization, $(\mu_n G_D)^2$, in the low Q^2 region from recent measurements. The solid triangle is the result from Ref. [2] with the total error being the quadrature sum of the statistical and systematic errors, the open diamonds are from Ref. [1] with the inner (outer) error bars being the statistical (total) uncertainties, the open stars are from Ref. [3] with the errors being the quadrature sum of the statistical and systematic errors, and the solid dot is the re-extracted value from Ref. [11] (see text) with the error shown as the quadrature sum of the statistical and systematic uncertainties.**

Because of the unique ground state spin structure of ^{3}He nucleus, polarized ^{3}He targets have proven to be very useful in studying the electric and magnetic form factors of the neutron and the spin structure of the neutron [13-16]. Recently, the neutron magnetic form factor at $Q^2 = 0.19$ (GeV/c)^2 was extracted for the first time from the inclusive spin-dependent quasi-elastic transverse asymmetry, $A_{T'}$ measured from the $^3\vec{H}e(\vec{e},e')$ reaction [11]. The published G_M^n value [11] was extracted based on plane wave impulse approximation (PWIA) calculations in which spin-dependent spectral functions were used [17-18]. While the agreement of the $A_{T'}$ data with the PWIA calculations of $A_{T'}$ is good, the agreements between the PWIA calculations of the ^{3}He transverse-longitudinal asymmetry $A_{TL'}$ and the data near the quasi-elastic peak [19] and in the low electron energy transfer region [20] are rather poor. This is largely because of the sensitivity of $A_{TL'}$ to the ^{3}He ground state structure as discussed in Ref. [19], and the sensitivities to final state interactions (FSI) and meson exchange currents (MEC) as well as the ^{3}He ground state structure for $A_{TL'}$ in the

low energy transfer region.

Recently, Ishikawa and Glöckle *et al.* [21] have performed new calculations of the ^{3}He inclusive spin-dependent quasi-elastic transverse asymmetry $A_{T'}$ in which final state interactions (FSI) were included. Fig. 3 shows the measured ^{3}He inclusive spin-dependent quasi-elastic transverse asymmetry $A_{T'}$ [11], as a function of the electron energy transfer, ω, together with the two PWIA calculations [17-18] and the calculation by Ishikawa *et al.* [21]. The deviation of the result by Ishikawa *et al.* [21] from those of PWIA calculations [17-18] is significant away from the quasi-elastic peak. The agreement between the data on $A_{T'}(\omega)$ and the calculation by Ishikawa *et al.* is excellent in terms of the size of the asymmetry and also the shape. Unfortunately, because of the large errors associated with the measured $A_{T'}(\omega)$ as shown in Fig. 3, it is not possible to put constraints on the theoretical calculations of the ^{3}He inclusive spin-dependent quasi-elastic asymmetry.

Because of the limitation of the statistics of the measurement, the measured quasi-elastic asymmetry, $A_{T'}(\omega)$, averaged over the experimental ω acceptance was used in extracting ${G_M^n}^2$ in Ref. [11]. The extracted value of ${G_M^n}^2$ at $Q^2 = 0.19$ (GeV/c)^2, based on PWIA calculations in which the spin dependent spectral functions were used, is $0.998 \pm 0.117 \pm 0.059$ [11] in unit of $(\mu_n G_D)^2$ with the uncertainties being the statistical and systematic, respectively. The neutron magnetic form factor at $Q^2 = 0.19$ (GeV/c)^2 has been re-extracted using the calculation by Ishikawa *et al.* [21]. The new value of ${G_M^n}^2$ in unit of $(\mu_n G_D)^2$ is $0.867 \pm 0.095 \pm 0.048$ and is shown in Fig. 2 as the solid circle. The new value of ${G_M^n}^2$ is different from the old value by 15%, which indicates that the effect of the FSI is not negligible at $Q^2 = 0.19$ (GeV/c)^2 for the inclusive transverse asymmetry $A_{T'}$. Thus, precise measurement of $A_{T'}(\omega)$ as a function of Q^2 is very important in terms of studying the FSI effect and also constraining theoretical calculations of the ^{3}He quasi-elastic asymmetry.

The uncertainty from model dependence in extracting the neutron magnetic form factor was studied carefully [11] following the approach by Friar *et al.* [22], and the uncertainty was determined to be 3% in ${G_M^n}^2$. Fig. 4 shows the sensitivity of $A_{T'}$ calculated by Ishikawa *et al.* [21] to different N-N interaction potentials. In Ref. [11] the measured quasi-elastic asymmetry, $A_{T'}(\omega)$, averaged over the experimental ω acceptance was used to extract ${G_M^n}^2$ because of the limitation of the statistics of the measurement. We propose in this experiment 2% statistical and 3% systematic uncertainties for $A_{T'}$ measurements on top of the ^{3}He quasi-elastic peak (20 MeV bin for the electron energy transfer) at all proposed values of Q^2. Therefore, the uncertainty from model dependence can be further reduced by using the precisely measured proton form factor data at the corresponding Q^2 of the proposed measurement for calculating $A_{T'}$ on top of the ^{3}He quasi-elastic peak. Though G_E^n is known rather poorly in the Q^2 region of this experiment, its contribution to $A_{T'}$ is negligible. The uncertainty in extracting G_M^n from model dependence using the calculations of Ishikawa *et al.* is estimated to be 1.0% based on the results for different N-N potentials. To emphasize, only $A_{T'}$ in close vicinity of the quasi-elastic peak ($\omega_0 - 10$ MeV $\leq \omega \leq \omega_0 + 10$ MeV) will be used in extracting G_M^n, a procedure expected to be much less sensitive to final state interactions, meson exchange currents, and relativistic effects. Currently, calculation of the ^{3}He inclusive spin-dependent quasi-elastic asymmetry which includes the final state interactions, meson exchange currents, and relativistic effects is underway [23]. Therefore, precise measurement of the ^{3}He $A_{T'}(\omega)$ is necessary to constrain theoretical calculations of $A_{T'}(\omega)$ to allow extracting G_M^n with high precision on top of the ^{3}He quasi-elastic peak.

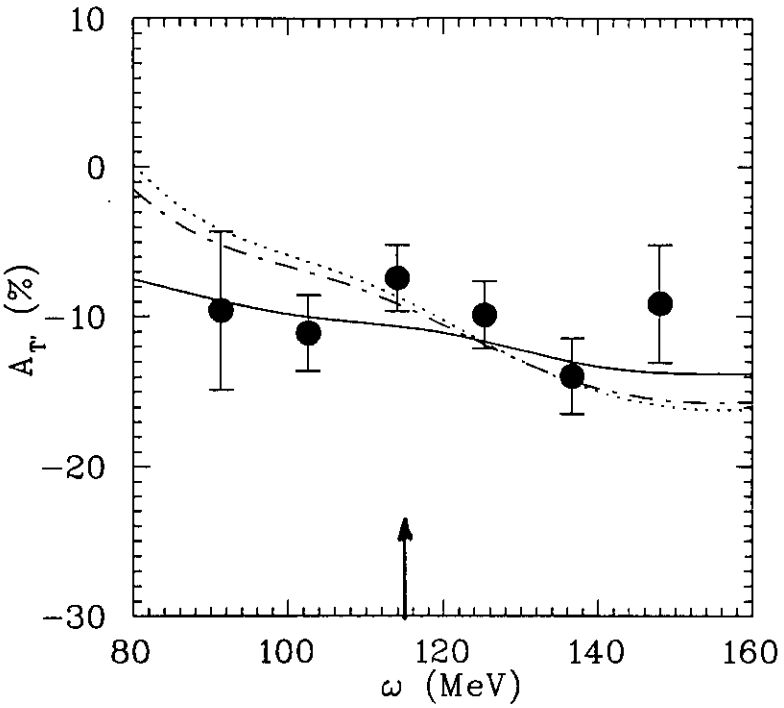

FIG. 3. **The transverse asymmetry $A_{T'}$ as a function of electron energy loss ω. The solid circles are the data points from Ref. [11] with statistical uncertainties only. The dotted line is the calculation by Salmè *et al.* [17], the dash-dotted line is the calculation by Schulze *et al.* [18], and the solid line is the calculation by Ishikawa *et al.* [21]. The quasi-elastic peak is indicated by the arrow.**

The physics motivation for this proposal is three-fold. First, precise measurements of the ^{3}He inclusive spin-dependent quasi-elastic transverse asymmetry will constrain theoretical calculations of the ^{3}He quasi-elastic asymmetry. $A_{T'}$ is the only inclusive spin-dependent asymmetry which is not sensitive to the small components of the ^{3}He ground state wave function. Thus, it is an excellent testing ground for three-body calculations. Secondly, precise measurements of the ^{3}He inclusive spin-dependent transverse quasi-elastic asymmetry, together with the improved theoretical calculation of the quasi-elastic asymmetry will allow us to extract the neutron magnetic form factor with high precision to resolve the discrepancy among the existing data sets. Lastly, the precise measurement of the Q^2-dependence of the neutron magnetic form factor at low Q^2 will serve as a benchmark for testing theoretical calculations of nucleon form factors at all momentum transfers.

Brook *et al.* [24] proposed CEBAF experiment E94-017 to measure G_M^n at Q^2 from 0.3 to 5.1 $(\mathrm{GeV/c})^2$ by measuring the cross section ratio of quasi-elastic electron-neutron to electron-proton scattering in deuterium. While this experiment will overlap with the approved Hall B experiment E94-017 [24] at $Q^2 = 0.3, 0.5$ $(\mathrm{GeV/c})^2$ with comparable precision on G_M^n measurements, the focus of this experiment is precision measurements of G_M^n at lower Q^2 and its Q^2 dependence. Furthermore, this experiment employs a different technique in which the spin degrees of freedom are used. This proposed experiment is also complementary to the Hall A approved experiment E93-024 [25] which will measure G_M^n at large Q^2

(1-6.5 $(\mathrm{GeV/c})^2$) by inclusive quasifree electron deuteron scattering.

In addition to the experiment we are proposing here in which a polarized ^{3}He target will be employed, there are two experiments approved at MIT-Bates and NIKHEF [26,27] using polarized ^{3}He targets from which information on G_M^n is expected in the same Q^2 region as this proposal. The MIT-Bates experiment proposed by Bernstein and Chupp [26] will measure the inclusive spin-dependent quasi-elastic asymmetry $A_{T'}$ at $Q^2 = 0.24, 0.45, 0.70$ $(\mathrm{GeV/c})^2$. The overall anticipated error in $A_{T'}$ measurement is 10%. The NIKHEF experiment [27] will measure the spin-dependent asymmetries from reaction $^3\vec{H}e(\vec{e}, eX)$ with X = 0, p, n, d, pn at $Q^2 = 0.15, 0.3, 0.5$ $(\mathrm{GeV/c})^2$ using an internal polarized ^{3}He target and the AmPS storage ring. Although information on G_M^n is expected from the inclusive measurement, the experiment is focused on the coincidence channels and especially the G_E^n measurement. The uncertainty in the inclusive $A_{T'}$ measurement is not expected to be able to compete with this experiment. We want to emphasize that the experiment we are proposing is the only experiment using a polarized ^{3}He target dedicated to measure the inclusive quasi-elastic transverse asymmetry, $A_{T'}$ precisely at low Q^2.

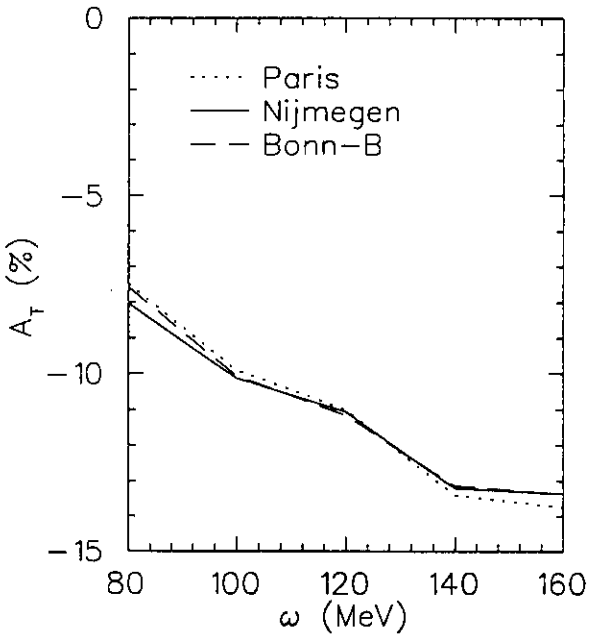

FIG. 4. **The transverse asymmetry $A_{T'}$ as a function of electron energy loss ω calculated by Ishikawa *et al.* [21] at the kinematics of the Bates experiment [11] for different N-N potentials with Gari-Krüpelmann nucleon form factor parametrization.**

The rest of the proposal is organized as follows: Section II contains a description of the inclusive ^{3}He spin-dependent quasi-elastic asymmetry and the elastic asymmetry; Section III describes the proposed experiment, in which the principle of the spin-exchange polarized ^{3}He target is discussed as well as the expected backgrounds and the systematic uncertainties associated with the asymmetry measurements; Section IV contains beam time request; Section V discusses the collaboration background and the responsibilities; and the last Section contains the acknowledgements.

II. ^{3}HE SPIN-DEPENDENT ASYMMETRIES

A. Spin-dependent Quasi-elastic Asymmetry from $^3\vec{H}e(\vec{e},e')$

The spin-dependent asymmetry for longitudinally polarized electrons scattered from a polarized spin-$\frac{1}{2}$ nuclear target can be written [28] as

$$A = -\frac{\cos\theta^* v_{T'} R_{T'} + 2\sin\theta^*\cos\phi^* v_{TL'} R_{TL'}}{v_L R_L + v_T R_T}, \tag{1}$$

where v_K are the kinematic factors defined in Ref. [28], and θ^* and ϕ^* are the polar and azimuthal angles of the target spin with respect to the 3-momentum transfer vector $\mathbf{q}$. $R_L(Q^2,\omega)$ and $R_T(Q^2,\omega)$ are the longitudinal and transverse nuclear response functions associated with the unpolarized cross section and are functions of the square of the 4-momentum transfer Q^2 and the electron energy loss ω. $R_{T'}(Q^2,\omega)$ and $R_{TL'}(Q^2,\omega)$ are the two response functions arising from the polarization degrees of freedom. $R_{T'}$ is a transverse response function and $R_{TL'}$ represents the interference between the transverse and the longitudinal multipoles. By orienting the target spin at $\theta^* = 0°$ or $\theta^* = 90°$, corresponding to the spin direction either along the 3-momentum transfer vector $\mathbf{q}$ or normal to it, one can select the transverse asymmetry $A_{T'}$ (proportional to $R_{T'}$) or the transverse-longitudinal asymmetry $A_{TL'}$ (proportional to $R_{TL'}$).

In the case of longitudinally polarized electrons scattering off a polarized nucleon target, the spin-dependent asymmetry is expressible in terms of the electric and magnetic form factors of the nucleon:

$$A_{\vec{e}\vec{N}} = -\frac{2\tau v_{T'}\cos\theta^* G_M^2(Q^2) + 2\sqrt{2\tau(1+\tau)}v_{TL'}\sin\theta^*\cos\phi^* G_M(Q^2)G_E(Q^2)}{(1+\tau)v_L G_E^2 + 2\tau v_T G_M^2}. \tag{2}$$

^{3}He is an interesting nucleus for polarization studies because its ground state wave function is predominantly a spatially symmetric S state ($\sim 90\%$) in which the spin of the nucleus is carried mainly by the neutron. For inclusive quasi-elastic scattering of the longitudinally polarized electrons from a polarized ^{3}He nucleus, the spin-dependent asymmetry can be written in the simplest impulse approximation model as:

$$A = \frac{A^{N=n}\sigma_n}{\sigma_n + 2\sigma_p}, \tag{3}$$

where $A^{N=n}$ is the asymmetry for elastic scattering of electrons off a free neutron target, and σ_n and σ_p are the elastic cross section of electrons scattering off a free neutron and a free proton targets, respectively. Thus, the ^{3}He inclusive spin-dependent quasi-elastic transverse asymmetry, $A_{T'}$, is most sensitive to the square of the neutron magnetic form factor, as can be seen easily from Eq. (2) and Eq. (3). This picture is confirmed by the PWIA calculations [17-18] in which the spin-dependent spectral functions were used and also confirmed by the recent measurement from MIT-Bates [11].

The experimental asymmetry will be diluted by the product of the beam and target polarizations. For the spin-exchange polarized ^{3}He target, the target would be filled with the "contaminants" $^{85}_{37}$Rb (72.165% of the natural Rb abundance) and $^{87}_{37}$Rb (27.835% natural

abundance) as well as $^{14}_{7}$N in the form of molecular nitrogen besides ^{3}He. Presently we assume a ^{3}He volume density of about 2.5×10^{20} atoms/cm^3, the Rb density will be on the order of 6×10^{14}/cm^3, and the nitrogen partial pressure will be about 100 torr or 1.4×10^{19}N/cm^3 at room temperature. The numbers combined result in a dilution factor of 0.94 for the ^{3}He nuclei.

B. ^{3}He Elastic Asymmetry

For longitudinally polarized electrons scattering elastically from a polarized ^{3}He nuclear target, the elastic asymmetry can be expressed in terms of the ^{3}He charge and magnetic form factors, F_c and F_m, as

$$A_{el} = \frac{\Delta}{\Sigma} = -\frac{2\tau\mu_A^2 v_{T'} \cos\theta^* F_m^2 + 2\sqrt{2\tau(1+\tau)}\mu_A Z v_{TL'} \sin\theta^* \cos\phi^* F_m F_c}{(1+\tau)Z^2 v_L F_c^2 + 2\tau\mu_A^2 v_T F_m^2} \tag{4}$$

where the form factors have been normalized to

$$F_c(Q^2 = 0) = F_m(Q^2 = 0) = 1. \tag{5}$$

In this formula Z is the nuclear charge, μ_A is defined in terms of the magnetic moment of ^{3}He as $(m_{\rm He}/m_n)\mu_{\rm He}$, and all other variables are kinematic factors defined in Ref. [28]. The experimental elastic asymmetry is diluted by the product of the beam and target polarizations. Thus, the product of the beam and target polarization can be determined from the measured elastic asymmetry using the measured ^{3}He elastic form factors.

III. THE EXPERIMENT

A. Overview

The experiment will employ a longitudinally polarized electron beam, a spin-exchange polarized ^{3}He target, and the Hall A HRS spectrometers. Quasi-elastic kinematics are chosen for the inclusive $^3\vec{H}e(\vec{e}, e')$ reaction. The single-arm measurement of the spin-dependent quasi-elastic transverse asymmetry will be performed by using the Hall A electron HRS spectrometer for detecting the quasi-elastically scattered electrons. The hadron HRS spectrometer will be dedicated for measuring the ^{3}He elastic asymmetry so as to serve as a beam and target polarization monitor. We propose to perform single-arm measurements from $^3\vec{H}e(\vec{e}, e')$ reaction at the quasi-elastic kinematics with an incident electron beam energies of 0.8 and 1.6 GeV, and at electron scattering angles of 20.8°, 23.6°, 24.5°, 28.01°, and 34.9°, covering a Q^2 region from 0.1 to 0.5 (GeV/c)^2, in steps of 0.1 (GeV/c)^2. The target spin direction will be aligned along the three-momentum transfer vector, q and the ^{3}He spin-dependent quasi-elastic transverse asymmetry, $A_{T'}(\omega)$ will be formed by varying the helicity of the polarized electron beam. The motivation for the choice of the beam energies was the resulting forward angles for the scattered electron in order to have the large effective target length acceptance for the spectrometer at the proposed kinematics, and also the convenience of energy change at CEBAF. The Hall A hadron spectrometer with a gas Cerenkov

counter will be employed as an excellent monitor of the beam and target polarizations for the proposed experiment.

We propose this experiment to be performed in Hall A for the following two reasons: the availability of a spin-exchange polarized ^{3}He target which will be built for the other Hall A proposed experiments in which a spin-exchange polarized ^{3}He target will be employed [29], and the 10-cm extended target length acceptance at 90° for both HRS spectrometers. Furthermore, this piece of physics will enrich the existing Hall A polarized ^{3}He program.

B. Polarized Electron Beam

Given the technical developments currently achieved with strained GaAs cathodes at SLAC (E143) and other places, high electron polarization (80%) is possible to achieve at CEBAF. Although the currents used in SLAC E-143 experiment were small (few tens of nanoamps), the newly approved experiment at 50 GeV (E-154) is planning to use similar value of polarization with few microamps average beam currents. SLAC is confident to achieve large electron polarization with high currents. We assume in this proposal the achievable electron polarization at CEBAF is 70% [30]. A beam current of 10 μA is chosen in this proposal because of the depolarization effect from the beam on the polarized ^{3}He target.

C. The Spin-Exchange Polarized ^{3}He Target

The polarized target will be based on the principle of spin exchange between optically pumped alkali-metal vapor and noble-gas nuclei [31-33]. The design will be similar in many ways to that used in E-142, an experiment at SLAC to measure the spin dependent structure function of the neutron [16]. A central feature of the target will be sealed glass target cells, which will contain a ^{3}He pressure of about 10 atmospheres. As indicated in Fig. 5, the cells will have two chambers, an upper chamber in which the spin exchange takes place, and a lower chamber, through which the electron beam will pass. In order to maintain the appropriate number density of alkali-metal (which will probably be Rb) the upper chamber will be kept at a temperature of 170–200° C using an oven constructed of the high temperature plastic Torlon. With a density of 2.5×10^{20} atoms/cm^3, and a lower cell length of 40 cm, the target thickness will be 1.0×10^{22} atoms/cm^2. We describe below in greater detail some features of the target.

1. Operating Principles

The time evolution of the ^{3}He polarization can be calculated from a simple analysis of spin-exchange and ^{3}He nuclear relaxation rates [34]. Assuming the ^{3}He polarization $P_{^3He} = 0$ at $t = 0$,

$$P_{^3He}(t) = < P_{Rb} > \left(\frac{\gamma_{SE}}{\gamma_{SE} + \Gamma_R}\right)\left(1 - e^{-(\gamma_{SE}+\Gamma_R)t}\right), \qquad (6)$$

where γ_{SE} is the spin-exchange rate per ^{3}He atom between the Rb and ^{3}He, Γ_R is the relaxation rate of the ^{3}He nuclear polarization through all channels other than spin exchange with Rb, and P_{Rb} is the average polarization of a Rb atom. Likewise, if the optical pumping is turned off at $t = 0$ with $P_{^3He} = P_0$, the ^{3}He nuclear polarization will decay according to

$$P_{^3He}(t) = P_0 e^{-(\gamma_{SE}+\Gamma_R)t}. \tag{7}$$

The spin exchange rate γ_{SE} is defined by

$$\gamma_{SE} = < \sigma_{SE} v > [Rb]_A, \tag{8}$$

where, $< \sigma_{SE} v >= 1.2 \times 10^{-19}$ cm^3/sec is the velocity-averaged spin-exchange cross section for Rb–^{3}He collisions [35-37] and $[Rb]_A$ is the average Rb number density seen by a ^{3}He atom. Our target will be designed to operate with $1/\gamma_{SE} = 8$ hours.

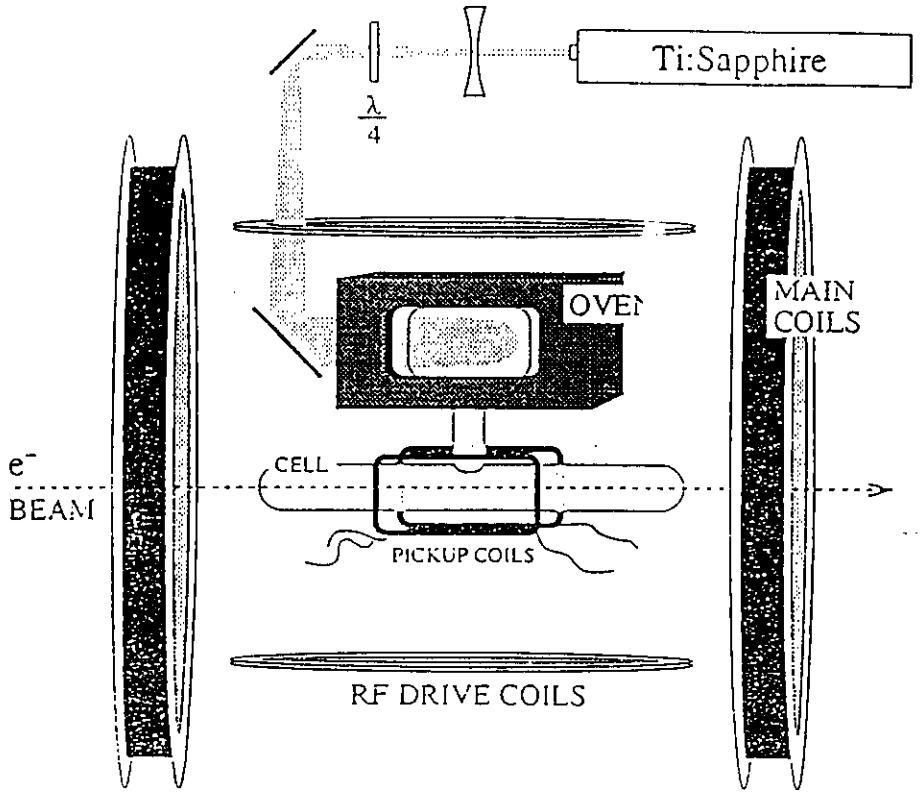

FIG. 5. **Schematics of the spin-exchange polarized ^{3}He target.**

From Eq. (6) it is clear that there are two things we can do to get the best possible ^{3}He polarization — maximize γ_{SE} and minimize Γ_R. But from Eq. (8) it is also clear that maximizing γ_{SE} means increasing the alkali-metal number density, which in turn means more laser power. The number of photons needed per second must compensate for the spin relaxation of Rb spins. In order to achieve $1/\gamma_{SE} = 8$ hours, we will require about 24 Watts

of usable laser light at a wavelength of 795 nm. We will say more about the source of laser light below.

The rate at which polarization is lost, which is characterized by Γ_R, will have four principle contributions. An average electron beam current of about 10 μA will result in a depolarization rate of $\Gamma_{beam} = 1/45$ hours [37]. Judging from experience at SLAC, we can produce target cells with an intrinsic rate of $\Gamma_{cell} = 1/50$ hours. This has two contributions, relaxation that occurs during collisions of ^{3}He atoms due to dipole-dipole interactions [38], and relaxation that is presumably due largely to the interaction of the ^{3}He atoms with the walls. Finally, relaxation due to magnetic field inhomogeneities can probably be held to about $\Gamma_{\Delta B} = 1/100$ hours [39]. Collectively, under operating conditions, we would thus expect

$$\Gamma_R = \Gamma_{beam} + \Gamma_{cell} + \Gamma_{\Delta B} = 1/45 \text{ hours} + 1/50 \text{ hours} + 1/100 \text{ hours} = 1/19 \text{ hours}. \quad (9)$$

Thus, according to Eq. 6, the target polarization cannot be expected to exceed

$$P_{max} = \frac{\gamma_{SE}}{\gamma_{SE} + \Gamma_R} = 0.70. \quad (10)$$

Realistically, we will not achieve a Rb polarization of 100% in the pumping chamber, which will reduce the polarization to about 40-45%.

2. Target Cells

The construction and filling of the target cells must be accomplished with great care if $1/\Gamma_{cell}$ is to be in excess of 50 hours. We plan to use the "Princeton Prescription" which was developed for use in SLAC E-142. This resulted, among the cells that were tested, in lifetimes that were always better than 30 hours, and in about 60% of the cells, better than 50 hours. The following precautions will be taken:

1. Cells will be constructed from aluminosilicate glass.

2. All tubing will be "resized." This is a process in which the diameter of the tubing is enlarged by roughly a factor of two in order to insure a smooth pristine glass surface that is free of chemical impurities.

3. Cells will be subjected to a long (4–7 day) bake-out at high ($> 400°$C) temperature on a high vacuum system before filling.

4. Rb will be doubly distilled in such a manner as to avoid introducing any contaminants to the system.

5. The ^{3}He will be purified either by getters or a liquid ^{4}He trap during filling.

The cells will be filled to a high density of ^{3}He by maintaining the cell at a temperature of about 20 K during the filling process. This is necessary so that the *pressure* in the cell is below one atmosphere when the glass tube through which the cell is filled is sealed. The length of the cell has been chosen to be 40 cm so that the end windows will not be within the acceptance of the Hall A spectrometers. The end windows themselves will be about 100 μ thick. Thinner windows could in principle be used, but this does not appear to be necessary.

3. The Optics System

As mentioned above, approximately 20–24 Watts of "usable" light at 795 nm will be required. By "usable," we essentially mean light that can be readily absorbed by the Rb. It should be noted that the absorption line of the Rb will have a full width of several hundred GHz at the high pressures of ^{3}He at which we will operate. Furthermore, since we will operate with very high Rb number densities that are optically quite thick, quite a bit of light that is not within the absorption linewidth is still absorbed.

It is our plan to take advantage of new emerging diode laser technology to economically pump the target. Systems are now commercially available in which a single chip produces about 20 watts of light, about half of which is probably usable. Between 2–4 such systems, at a cost of about $25,000 each, should do the job. There is also a group a Lawrence Livermore Laboratory that has offered to build us a single chip that can produce 150 watts. While some studies of the use of diode lasers for spin-exchange optical pumping do exist in the literature [40], actual demonstrations of high polarizations in cells suitable for targets are much more recent [41]. For the recently finished SLAC experiment E154, the diode laser system was used for the spin exchange polarized ^{3}He target.

4. Polarimetry

Polarimetry will be accomplished by two means. During the experiment, polarization will be monitored using the NMR technique of adiabatic fast passage (AFP) [42]. The signals will be calibrated by comparing the ^{3}He NMR signals with those of water. The calibration will be independently verified by studying the frequency shifts that the polarized ^{3}He nuclei cause on the electron paramagnetic resonance (EPR) lines of Rb atoms. This second techniques will be performed in separate target studies, not during the experiment. For this experiment we will use the hadron HRS spectrometer as beam and target polarization monitor, the NMR technique of the target polarization measurement will be used as cross check.

5. Apparatus Overview

The target will be in air or, perhaps, in a helium bag. This greatly simplifies the design. The main components of the target are shown in Fig. 5. The "main coils" shown are large Helmholtz coils that will be used to apply a static magnetic field of about 20 Gauss. In addition to establishing the quantization axis for the target, the main coils are important for suppressing relaxation due to magnetic field inhomogeneities, which go like $1/B^2$. At 20 G, inhomogeneities can be as large as about 30 mG/cm while keeping $\Gamma_{\Delta B} < 1/100$ hours. By increasing the applied field to about 40 G, and relaxing our requirements on $\Gamma_{\Delta B}$ by about factor of two, inhomogeneities as large as 0.25 G/cm can be tolerated. We are still finalizing our final choice of static field.

The NMR components in the target include a set of RF drive coils, and a separate set of pick-up coils. Not shown in the figure are the NMR electronics, which include an RF power amplifier, a lock-in amplifier, some bridge circuitry, and the capability to sweep the static magnetic field. The oven shown in Fig. 5 is constructed of Torlon, a high temperature

plastic. The oven is heated with forced hot air. The optics system will either include five Ti:sapphire lasers (only one is shown) or 2–4 laser diode systems. Either way, there will also be several lenses and a quarter wave plate to provide circular polarization.

D. The Spectrometers

The two Hall A HRS spectrometers will be used for this experiment, with the electron HRS spectrometer in its standard configuration for detecting the quasi-elastically scattered electrons and the hadron HRS spectrometer for detecting the elastically scattered electrons from the ^{3}He target. The pion rejection from the electron by the combination of a gas Cerenkov counter and a shower counter in the electron HRS spectrometer is more than that is required for this experiment. The gas Cerenkov counter in the hadron HRS spectrometer will provide adequate pion rejection for detecting the elastically scattered electrons. The most forward scattering angle for the electron HRS spectrometer is 20.8° and the maximum sacttering angle for it is 34.9°. The hadron HRS spectrometer will be fixed at one angle for each of the beam energies (24° for 0.8 GeV and 16° for 1.6 GeV). The highest singles rate in the electron HRS spectrometer is 6.1 KHz and the highest singles rate in the hadron spectrometer is 2.2 KHz, which are much lower than the designed 10 KHz data acquisiton rate for Hall A. The central momentum and angle settings corresponding to the top of the quasi-elastic peak for the electron arm spectrometer are listed in Table I. A 10% momentum acceptance of the spectrometer will cover an adequate electron energy loss region on both sides of the quasi-elastic peak to provide precise measurements of $A_{T'}(\omega)$ at all Q^2 proposed so as to constrain theoretical calculations of $A_{T'}(\omega)$.

E. Background

At all the kinematics for detecting the quasi-elastically scattered electrons (electron HRS) and the elastically scattered electrons (hadron HRS), the electro-produced pion rates are negligible compared with the expected electron rates ($\leq 1\%$). Furthermore, both spectrometers are equipped with gas Cerenkov counters, so pion background is not a concern for this experiment. As was discussed earlier, the target would be filled with the "contaminants" $^{85}_{37}$Rb (72.165% of the natural Rb abundance) and $^{87}_{37}$Rb (27.835% natural abundance) as well as $^{14}_{7}$N in the form of molecular nitrogen, so "empty target", i.e. without ^{3}He in the target, background studies will be performed at all proposed kinematics before the experiment during the checkout.

F. Systematic Uncertainties

We aim at a 2% statistical accuracy for $A_{T'}$ on top of the ^{3}He quasi-elastic peak at all the Q^2 points proposed. So as not to limit our data by the systematic uncertainties associated with the determinations of the beam and target polarizations using the Möller polarimeter (beam) and the NMR measurement (target), we propose to use the hadron HRS spectrometer as a monitor of the beam and target polarizations constantly during the experiment. The ^{3}He elastic charge and magnetic form factors at $Q^2 = 0.1, 0.2$ (GeV/c)^2

were determined by Rosenbluth separation [43] to overall uncertainties of 1.5%. Thus, by precisely measuring the elastic asymmetry at $Q^2 = 0.1, 0.2$ $(\mathrm{GeV/c})^2$, the product of the beam and target polarizations can be determined to an overall uncertainty of 3%. As cross check the beam polarization will be measured during the experiment using the Moller polarimeter and the target polarization will also be monitored using the NMR technique.

For helicity-dependent asymmetry measurements, any helicity-correlated variation in the system will cause a systematic uncertainty in the measured asymmetry. If there is a helicity-correlated beam charge difference for the beam pulse, there will be an asymmetry contribution to the experimental asymmetry from the helicity-correlated beam energy shift due to the beam loading effect, as the physical cross section is energy dependent. The empty target background might be dependent on the beam position, which will be studied carefully before the experiment. If there were helicity-correlated beam motion, then there would be an asymmetry contribution to the measured asymmetry from this beam motion as the empty target yield would be different for each of the electron helicities. False asymmetries from helicity-correlated beam current shift, beam motion, as well as the detector efficiency change need to be addressed carefully.

For the Bates experiment 88-25 [11], all these effects were studied very carefully. The average helicity-correlated current shift weighted by the beam charge in each run is $\frac{\Delta I}{I} = 23.3 \pm 324.6$ ppm. The total accumulated beam charge for this analysis is 26.2 Coulombs. The average beam peak current during the experiment was around 2.5 mA; the size of the contribution to the measured asymmetry from this helicity-correlated beam current variation has been estimated to be approximately four orders of magnitude smaller than the measured quasi-elastic asymmetry. The average helicity-correlated beam motion from analyzing all the beam position monitor data is -0.20 ± 1.06 μ m for the x position and 0.08 ± 1.14 μ m for the y position. The calculated asymmetry contributions due to the helicity-correlated beam motion are approximately four orders of magnitude smaller than the measured asymmetry. The weighted average of the relative drift chamber efficiency variation is $0.03 \pm 0.90\%$ for the full target runs, and $-1.34 \pm 4.82\%$ for the empty target runs, and again the false asymmetry from the helicity-correlated detector efficiency change is negligible compared with the measured asymmetry. Although the Bates machine has a duty factor of 1% operated at 600 Hz with flipping of the electron helicity on the pulse-by-pulse basis, a helicity flipping rate of 30 Hz is anticipated at CEBAF. Thus, from the analysis shown above from the Bates experiment, we do not expect to have significant systematic uncertainties associated with helicity-correlated effects for this experiment. From the Bates experiment [11], the overall systematic uncertainty of the $A_{T'}$ measurement is dominated by the uncertainties in determining the beam and target polarizations. The overall systematic uncertainty in $A_{T'}$ measurement is expected to be 3%.

IV. BEAM TIME REQUEST

In calculating the ^{3}He quasi-elastic cross section, we used the y-scaling calculation [44] which describes the quasi-elastic cross section as the product of a kinematic factor, a single-nucleon cross section, and a universal scaling function of the scaling variable y. The extracted spin-averaged quasi-elastic cross sections from the Bates experiment 88-25 [11] agree well with the y-scaling calculation [44], and also agree within $\pm 5\%$ with the measured cross

sections [45] scaled to its kinematics. The ^{3}He quasi-elastic asymmetry was calculated by Ishikawa *et al.* [21]. In calculating the rates, a target volume density of 2.5×10^{20} atoms/cm^3, a solid angle of 7 msr, together with a 10% spectrometer momentum bite were used. The effective target length acceptance by the spectrometer is 10 cm/ $\sin(\theta)$, where θ is the electron scattering angle. In estimating the beam time, we assumed 70% for the beam polarization, 40% for the target polarization, 0.94 for the dilution factor for the ^{3}He nuclei, and 90% for the detection efficiency. Table II lists the beam time in hours for all the kinematics which results in a relative statistical uncertainty of 2% for $A_{T'}$ on top of the quasi-elastic peak (a bin size of 20 MeV for the electron energy transfer, ω). Fig. 6 shows the proposed measurements of $A_{T'}(\omega)$ with the anticipated statistical errors, together with the calculation by Ishikawa *et al.* [21] at proposed Q^2. Fig. 7 shows the recent data on G_M^n at low Q^2 together with the anticipated results on G_M^n from this experiment, with the total errors being the quadrature sum of the statistical, systematic, and model dependence uncertainties.

For the elastic asymmetry measurements, the hadron spectrometer will be employed to detect the elastically scattered electrons. Table III lists the kinematics settings for the ^{3}He elastic peak at beam energies of 0.8 and 1.6 GeV. At the kinematics chosen for the elastic asymmetry measurements, the ^{3}He elastic peak is well separated from the elastic peaks from nitrogen and Rb. Therefore, the experimental ^{3}He elastic asymmetry is only diluted by the product of the beam and target polarizations. The elastic rates for electron beam current of 10μA and the beam time corresponding to 1% and 1.5% statistical uncertainties of the elastic asymmetry measurements are also listed in Table III. Again, we assumed 40% for the target polarization, 70% for the beam polarization, and 90% for the detection efficiency. To emphasize, no additional beam time is needed for the elastic asymmetry measurements because the data will be taken simultaneously with the quasi-elastic asymmetry measurements to monitor the beam and target polarizations.

So we request 217 hours for the ^{3}He quasi-elastic asymmetry measurements. In addition, we request 40 hours for the "empty" target studies, and an overhead of 50 hours for the beam energy change, beam polarization measurements, the spectrometer angle changes, and the target polarization alignments. In addition, we request two days of beam time for checkout. Thus, in total we request 355 hours (15 days) of beam time. This beam time estimate includes no contingency factor for the accelerator or spectrometer operation.

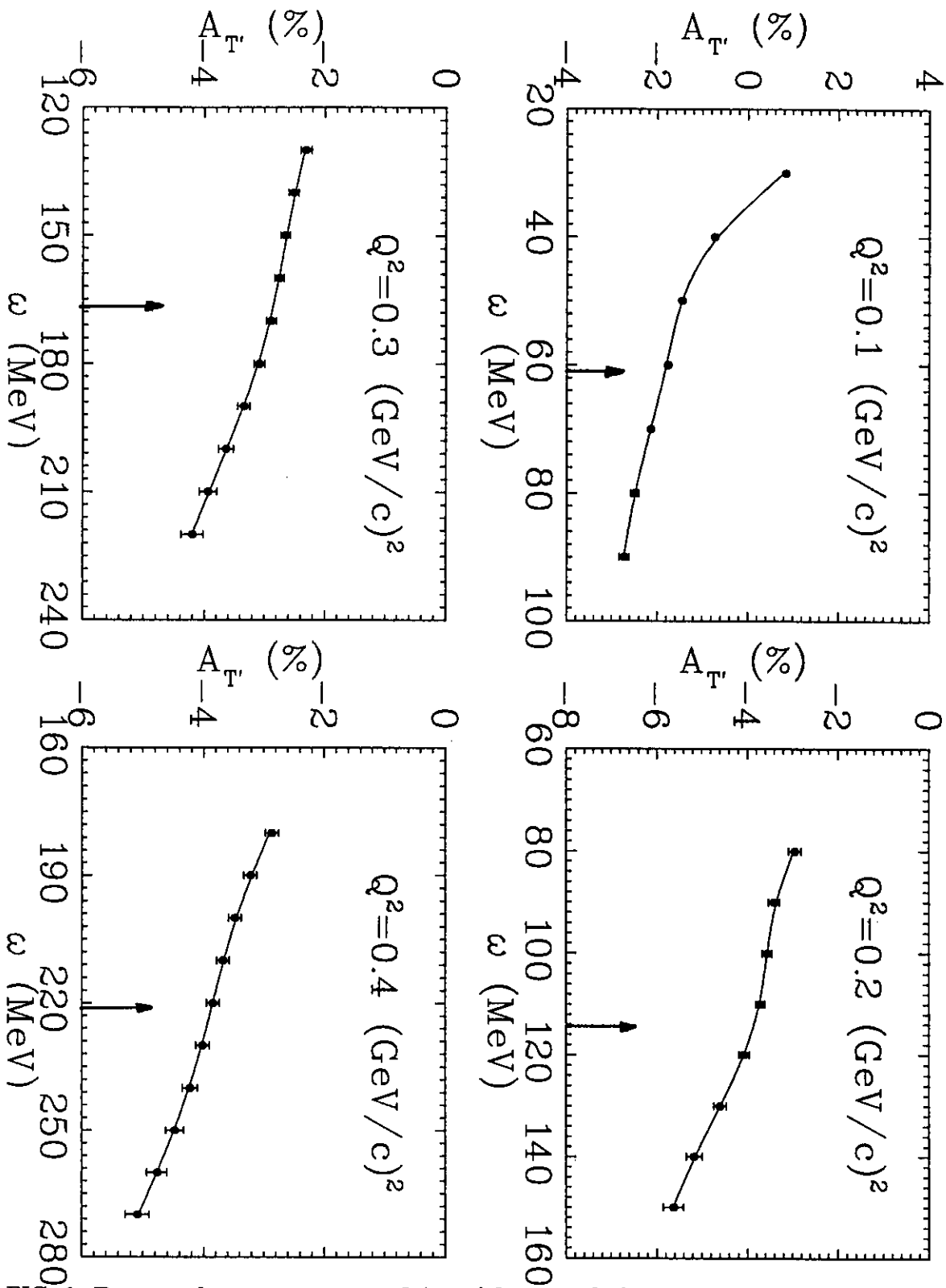

FIG. 6. **Proposed measurements of $A_{T'}$ with errors being the statistical uncertainties at proposed Q^2, together with the calculations by Ishikawa *et al.* [21]. The quasi-elastic peak is indicated by the arrow for each kinematics.**

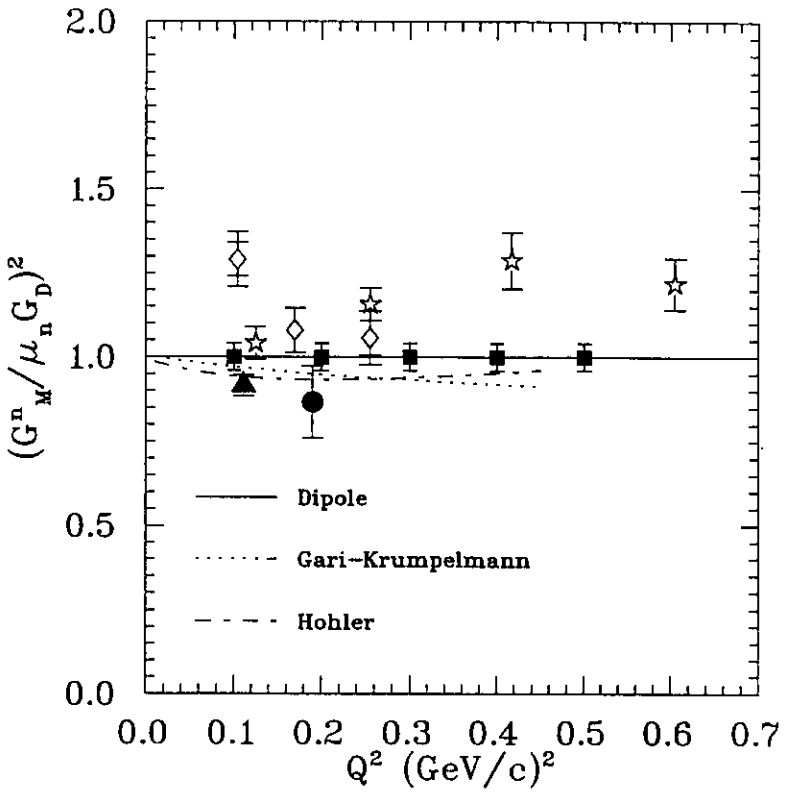

FIG. 7. **The square of the neutron magnetic form factor $G_M^n{}^2$, in units of the standard dipole parametrization, $(\mu_n G_D)^2$, in the low Q^2 region. The anticipated $(G_M^n)^2$ values from this proposal are shown as solid squares with the total errors being the quadrature sum of the statistical, systematic, and model dependence uncertainties.**

V. COLLABORATION BACKGROUNDS AND RESPONSIBILITIES

This experiment requires a spin-exchange polarized ^{3}He target and longitudinally polarized electron beam at a relatively low beam current (10μA), no special equipment outside of that proposed in the Hall A CDR is required. The spin-exchange polarized ^{3}He target will be provided by this collaboration which includes: Helmholtz coils for the holding field and the target polarimeter. Many members of this collaboration were involved significantly in the SLAC E142 experiment and the Bates 88-02 and 88-25 experiments in which polarized ^{3}He targets were employed. Also a significant fraction of this collaboration is involved in the on-going HERMES and the SLAC E154 experiments. This collaboration has much experience in running experiments with polarized electron beam and polarized ^{3}He targets. We request from CEBAF the beam pipe instrumentation, i.e. beam position and beam current monitors, as well as support from CEBAF for the target installation.

VI. ACKNOWLEDGEMENTS

We thank S. Ishikawa for timely calculations of $A_{T'}(\omega)$ at the proposed kinematics of this proposal, and V.R. Pandharipande, W. Glöckle, and T.-S.H. Lee for stimulating discussions and helpful comments.

REFERENCES

[1] P. Markowitz *et al.*, Phys. Rev. **C48**, R5 (1993).

[2] H. Anklin *et al.*, Phys. Lett. **B336**, 313 (1994).

[3] E.E.W Bruins *et al.*, Phys. Rev. Lett. **75**, 21 (1995).

[4] E.B. Hughes, T.A. Griffy, M.R. Yearian, and R. Hofstadter, Phys. Rev. **139**, B458 (1965); *ibid.* **146**, 973 (1966).

[5] D. Braess and G. Kramer, Z. Phys. **189**, 242 (1966); D. Braess, D. Hasselman n and G. Kramer, Z. Phys. **198**, 527 (1967); D. Hasselmann and G. Kramer, DE SY 67/21 (September 1967).

[6] B. Grossetête, S. Jullian, and P. Lehmann, Phys. Rev. **141**, 1435 (1966).

[7] K.M. Hanson, J.R. Dunning, Jr., M. Goitein, T. Kirk, L.E. Price, and Richard Wilson, Phys. Rev. **D8**, 753 (1973).

[8] R.J. Budnitz *et al.*, Phys. Rev. **173**, 1357 (1968).

[9] W. Bartel *et al.*, Phys. Lett. **30B**, 285 (1969); *ibid.* **39B** , 407 (1972); Nucl. Phys. **B58**, 429 (1973).

[10] P. Stein, M. Binkley, R. McAllister, A. Suri, and W. Woodward, Phys. Rev. Lett. **16**, 592 (1966).

[11] H. Gao *et al.*, Phys. Rev. **C50**, R546 (1994), H. Gao, Ph.D. thesis, California Institute of Technology (unpublished,1994).

[12] M.J. Musolf, T.W. Donnelly, J. Dubach, S.J. Pollock, S. Kowalski, and E.J. Beise, Phys. Report 239 (1,2), 1994.

[13] C.E. Woodward *et al.*, Phys. Rev. Lett. **65**, 698 (1990).

[14] A. K. Thompson *et al.*, Phys. Rev. Lett. **68**, 2901 (1992).

[15] M. Meyerhoff *et al.*, Phys. Lett. **B327**, 201 (1994).

[16] P.L. Anthony *et al.*, Phys. Rev. Lett. **71**, 959 (1993).

[17] C. Ciofi degli Atti, E. Pace, and G. Salmè, Phys. Rev. **C46**, R1591 (1992); C. Ciofi degli Atti, E. Pace and G. Salmè, in *Proceedings of the 6th Workshop on Perspectives in Nuclear Physics at Intermediate Energies*, ICTP, Trieste May 1993, (World Scientific); C. Ciofi degli Atti, E. Pace and G. Salmè, Phys. Rev. **C51**, 1108 (1995); G. Salmè, private communication.

[18] R.-W. Schulze and P.U. Sauer, Phys. Rev. **C48**, 38 (1993); R.-W. Schulze, private communication.

[19] J.-O. Hansen *et al.*, Phys. Rev. Lett. **74**, 654 (1995).

[20] C.E. Jones *et al.*, Phys. Rev. **C52**, 1520 (1995).

[21] S. Ishikawa and W. Glöckle, private communications.

[22] J.L. Friar, B.F. Gibson, G.L. Payne, A.M. Bernstein, and T.E. Chupp, Phys. Rev. **C42**, 2310 (1990).

[23] W. Glöckle, and J. Golak, private communication.

[24] CEBAF proposal E94-017, W. Brooks, spokesperson.

[25] CEBAF proposal E93-024, J. Gomez and G.G. Petratos, spokespersons.

[26] Update on MIT-Bates proposal 88-25 by A. Bernstein and T.E. Chupp (1994).

[27] NIKHEF electron-scattering proposal 94-05, J.F.J. van den Brand, spokesperson.

[28] T.W. Donnelly and A.S. Raskin, Ann. Phys. **169**, 247 (Academic Press, New York, 1986).

[29] CEBAF experiment E-94-010, G. Cates and Z.-E. Meziani, spokespersons; CEBAF proposal PR-94-020, W. Korsch, R. McKeown, and Z.-E. Meziani, spokespersons; CEBAF proposal PR-94-021, W. Korsch and R. McKeown, spokespersons; CEBAF proposal PR-94-101, Z.-E. Meziani and P.A. Souder, spokespersons.
[30] L.S. Cardman and C.K. Sinclair, CEBAF memo (1993).
[31] M.A. Bouchiat, T.R. Carver and C.M. Varnum, Phys. Rev. Lett. **5**, 373 (1960).
[32] N.D. Bhaskar, W. Happer, and T. McClelland, Phys. Rev. Lett. **49**, 25 (1982).
[33] W. Happer, E. Miron, S. Schaefer, D. Schreiber, W.A. van Wijngaarden, and X. Zeng, Phys. Rev. A **29**, 3092 (1984).
[34] T.E. Chupp. M.E. Wagshul, K.P. Coulter, A.B. McDonald, and W. Happer, Phys. Rev. **C36**, 2244 (1987).
[35] K.P. Coulter *et al.*, Nucl. Inst. Meth. in Phys. Res. **A270**, 90 (1988).
[36] N.R. Newbury *et al.*, Phys. Rev. **A48**, 558 (1993).
[37] K.P. Coulter *et al.*, Nucl. Inst. Meth. in Phys. Res. **A276**, 29 (1989).
[38] N.R. Newsbury *et al.*, Phys. Rev. **A48**, 4411 (1993).
[39] G.D. Cates *et al.*, Phys. Rev. **A38**, 5092 (1988).
[40] M.E. Wagshul and T.E. Chupp, Phys. Rev. **A40**, 4447 (1989).
[41] Private communication, Bill Cummings (1994).
[42] A. Abragam, *Principles of Nuclear Magnetism* (Oxford University Press, New York, 1961).
[43] A. Amroun *et al.*, Phys. Rev. Lett. **69**, 253 (1992); A. Amroun *et al.*, Nucl. Phys. **A579**, 596 (1994).
[44] G.B. West, Phys. Rep. **18C**, 264 (1975).
[45] K. Dow *et al.*, Phys. Rev. Lett. **61**, 1706 (1988); K. Dow, MIT Ph.D. thesis, 1987 (unpublished).

TABLES

E (GeV)	E' (GeV)	θ (degree)	θ_q (degree)	Q^2 $(\mathrm{GeV/c})^2$
0.8	0.746	23.6	-68.84	0.1
0.8	0.694	34.93	-59.76	0.2
1.6	1.440	20.79	-63.62	0.3
1.6	1.387	24.51	-59.57	0.4
1.6	1.334	28.01	-56.00	0.5

TABLE I. **Kinematics for the quasi-elastic $^3\vec{H}e(\vec{e},e')$ reaction. θ_q is the angle between the three-momentum transfer vector, $\vec{q}$ and the incident electron beam direction. The negative sign indicates that it is on the other side of the beam line compared with the scattered electron direction.**

E (GeV)	Q^2 $(\mathrm{GeV/c})^2$	I (μA)	Rate (Hz)	A (%)	$\frac{\Delta A}{A}$	Time (hrs)
0.8	0.1	5.0	6114.0	-1.76	0.02	27.0
0.8	0.2	10.0	795.0	-3.89	0.02	32.0
1.6	0.3	10.0	3195.0	-2.88	0.02	29.0
1.6	0.4	10.0	877.0	-3.85	0.02	54.0
1.6	0.5	10.0	373.0	-4.90	0.02	75.0

TABLE II. **The estimated $^3\vec{H}e(\vec{e},e')$ quasi-elastic rates and the beam time for all the Q^2 points proposed. 40% for the target polarization, 70% for the beam polarization, 0.94 for the dilution factor, and 90% of detector detection efficiency were assumed in the beam time estimation.**

E (GeV)	E' (GeV)	θ (degree)	Q^2 $(GeV/c)^2$	Rate (Hz)	$\frac{\Delta A}{A}$	Time (hrs)
0.8	0.781	24.0	0.10	2270.0	0.01	4.1
1.6	1.566	16.0	0.20	602.0	0.015	6.9

TABLE III. **The kinematics, rates and beam time for ^{3}He elastic asymmetry measurements. An electron beam current of 10 μA, a target polarization of 40%, a beam polarization of 70%, and a detection efficiency of 90% were assumed in the rates and beam time calculations.**